Final Report

STUDY OF ZERO-G PROPELLANT GAUGING BASED ON TANK ELECTROMAGNETIC RESONANCES

By: A. J. BAHR A. KARP

Prepared for:

GEORGE C. MARSHALL SPACE FLIGHT CENTER
NATIONAL AERONAUTICS AND SPACE ADMINISTRATION
MARSHALL SPACE FLIGHT CENTER, ALABAMA 35812

CONTRACT NAS8-31191

STANFORD RESEARCH INSTITUTE
Menlo Park, California 94025 · U.S.A.

STANFORD RESEARCH INSTITUTE
Menlo Park, California 94025 · U.S.A.

Final Report *April 1975*

Covering the Period 13 November 1974 to 21 February 1975

STUDY OF ZERO-G PROPELLANT GAUGING BASED ON TANK ELECTROMAGNETIC RESONANCES

By: A. J. BAHR A. KARP

Prepared for:

GEORGE C. MARSHALL SPACE FLIGHT CENTER
NATIONAL AERONAUTICS AND SPACE ADMINISTRATION
MARSHALL SPACE FLIGHT CENTER, ALABAMA 35812

CONTRACT NAS8-31191

SRI Project 3854-

Approved by:

DON PARKER, *Director*
Electromagnetic Techniques Laboratory

RAY L. LEADABRAND, *Executive Director*
Electronics and Radio Sciences Division

Copy No. 18

ABSTRACT

The results of an evaluation study of an RF mass gauging system currently under development by the Instruments and Life Support Division of the Bendix Corporation are presented. The potential limitations of such a system are determined and possible modifications in system design and measurement technique are discussed. In addition, an improved mathematical model for predicting the gauging response of the system is developed.

ACKNOWLEDGMENTS

The authors would like to acknowledge the important contributions of Mr. A. Rosengreen, who suggested the use of Fermi statistics for analyzing the mode counting problem, and Dr. C.M. Ablow, who worked out the detailed integration of the resulting mode density function. We also would like to thank Dr. D. Passeri and his staff at the Instruments and Life Support Division of the Bendix Corporation, Davenport, Iowa, for their complete cooperation in providing technical information about their RF mass gauging system.

CONTENTS

APPENDICES

ILLUSTRATIONS

I INTRODUCTION AND SUMMARY OF RESULTS

A. Introduction

This final report presents the results of a study to evaluate a RF mass gauging system that is currently under development by the Instruments and Life Support Division of the Bendix Corporation, Davenport, Iowa, Specifically, the study was divided into two major tasks:

(1) Establish the potential limitations and deficiencies of the RF gauging concept.

(2) Consider and recommend possible modifications in system design and measurement techniques.

There were two main sources of information that were used in this study: (a) the reports that have been issued by Bendix, and (b) discussions with Bendix personnel via telephone and during a visit by SRI personnel to the Bendix plant.

The essential elements of the RF gauging system are shown in the block diagram of Figure 1. The fundamental concept is simple: If the cavity is large enough compared with a wavelength, it will support many resonant electromagnetic modes. Thus, if the frequency is swept through a band, energy will be reflected from the cavity for frequencies where no resonance exists, and will be partially absorbed at any resonant frequency. Thus, there will be a dip in reflected power as each resonant frequency is traversed. (The amount of energy absorbed and the size of the dip will depend on the losses in the cavity and the degree of coupling to the cavity.) In principle, the number of dips in reflected power in a given frequency band will be a measure of the number of cavity

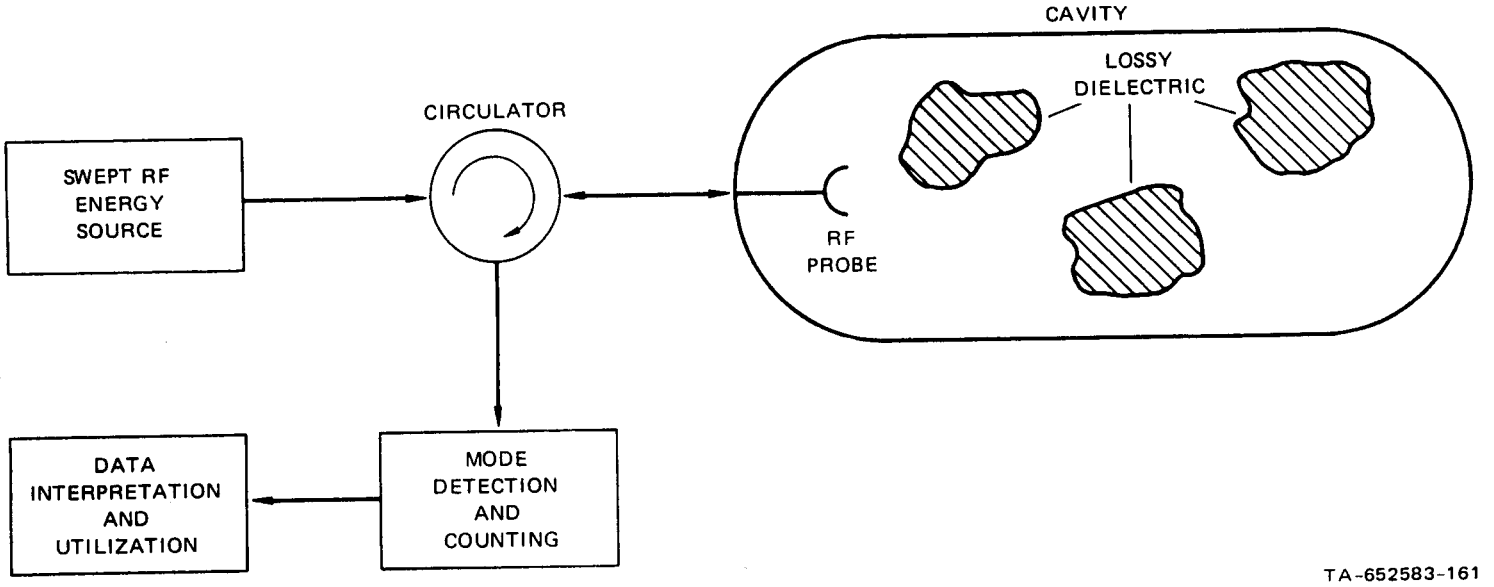

FIGURE 1 RF GAUGING SYSTEM

resonances in that band. Finally, the number of cavity resonances in a given band will depend on the amount of dielectric material in the cavity. Thus, it should be possible to calibrate the system so that the amount (volume) of dielectric in the cavity can be measured in terms of the number of dips in reflected power that are observed in a given frequency band.

However, in practice, a number of factors complicate the utilization of this system. The most important of these factors is the loss in the system, and the effect of variations in this loss with frequency and with the amount of dielectric material in the cavity. Therefore, a major part of the first task of this study involved examining the correctness and completeness of the math model that has been used by Bendix to analyze the effect of loss in the system. Section II of this report discusses this math model in detail and describes our suggested modifications.

In Section III, other important practical aspects of the system are considered and evaluated. These include resonator coupling, resonator geometry, and the effects of fuel movement, temperature, perturbations in the cavity, and so on. Finally, our overall conclusions and recommendations are presented in Section IV.

B. Summary of Results

The major results and conclusions of this study are:

- The technique of fuel gauging by means of counting modes of electromagnetic resonance in a large conducting cavity appears to be both valid and feasible, provided that it is used with a clear understanding of its limitations.

- The design and implementation of the current fuel-gauging system being developed by Bendix, does, in general, follow the basic tenets of good microwave

practice. However, a few recommendations for improvement are made.

- The exact configuration and geometry of a truly-large cavity should not have a significant effect on system performance. In particular, the introduction of perturbations into the cavity should not alter the average number of degeneracies and the exact location of the coupling probe should not matter.

- The "space-diversity" probe being used by Bendix is a good way to couple to the greatest number of modes, but care must be taken in processing the resulting data to avoid erroneous mode counts.

- An improved mathematic model for the fuel-gauging system has been developed and its limitations assessed. The model should provide a good basis for design, but it is probably not accurate enough to obviate the necessity for experimentally calibrating the actual fuel-gauging system.

II MATH MODEL

A. Introduction

In this section, we discuss a mathematical theory for determining the number of modes (resonances) in an electromagnetic cavity that are detectable (observable) between frequencies f_1 and f_2, where the cavity may contain an arbitrary amount of lossy dielectric material. The theory must necessarily be approximate because, in general, the cavity is asymmetrical and contains objects (perturbations) having complex geometries; thus, exact mathematical solutions cannot be obtained in closed form. The key assumption upon which the validity of this approximate analysis rests is that all major dimensions of the cavity are much larger than the electromagnetic wavelength. If this is true, the density of modes per unit frequency will be large and will be insensitive to the detailed boundary conditions in the cavity.

B. Density of Observable Modes--Lossless Case

Given the "large-cavity" assumption, an equation for the density of modes in a lossless cavity can be derived as follows: we assume that the cavity is a rectangular parallelepiped having sides L_x, L_y, L_z. (As mentioned before, the results should not depend on the exact shape of the cavity.) Since the tangential electric field must be zero at the cavity walls, the wave vector in any Fourier (plane-wave) decomposition of the modal fields must have a corresponding periodicity, that is

$$\vec{k} = \hat{a}_x \frac{2\pi n_x}{L_x} + \hat{a}_y \frac{2\pi n_y}{L_y} + \hat{a}_z \frac{2\pi n_z}{L_z} \quad , \qquad (1)$$

where $\vec{k}$ is the wave vector, $\hat{a}_x$, $\hat{a}_y$, $\hat{a}_z$ are orthogonal unit vectors, and

$$n_{x,y,z} = 0, \pm 1, \pm 2, \ldots \quad . \tag{2}$$

Now, since there are always two orthogonal polarizations possible for each set of integers (n_x, n_y, n_z), there are two independent modes for each "unit" cell in k-space, where the cell volume is given by $(2\pi)^3/L_x L_y L_z$. Thus, the number of modes between k and k + dk, where $k = |\vec{k}|$, is equal to twice the number of "unit" cells that make up the shell volume between spheres in k-space having radii k and k + dk. Expressing this relation mathematically, we have

$$\rho_1(k)dk = 2 \times \frac{4\pi}{3} [(k + kd)^3 - k^3]/[(2\pi)^3/L_x L_y L_z] \quad ,$$

or

$$\rho_1(k)dk = \frac{V}{\pi^2} k^2 \, dk \quad , \tag{3}$$

where $\rho_1(k)$ is the density of modes per unit wave number and $V = L_x L_y L_z$ is the volume of the cavity. To express this relation in the frequency domain, we use the fact that $k = 2\pi f/c$ and obtain

$$\rho_2(f)df = \frac{8\pi V}{c^3} f^2 df \quad , \tag{4}$$

where f is the frequency, c is the velocity of light, and $\rho_2(f)$ is the density of modes per unit frequency. Equation (4) is known as the "Hohlraum" formula in physics, where it occupies a fundamental place in the analysis of black-body radiation.

We now wish to generalize Eq. (4) one step further so that it includes the effect of a dielectric material that partially occupies the cavity volume. To show the explicit dependence of Eq. (4) on dielectric constant we rewrite it as follows:

$$\rho_2(f)df = \frac{8\pi V}{c_0^3} (\epsilon')^{3/2} f^2 df \quad , \tag{5}$$

where c_0 is the velocity of light in vacuum and ϵ' is the real part of the relative dielectric constant of the dielectric material filling the cavity. If only a fraction, α, of the volume is filled with dielectric material, ϵ' in Eq. (5) must be replaced by $\epsilon'(\alpha)$, an effective dielectric constant. One way to determine this effective dielectric constant is to assume that the total mode density for the cavity is the sum of two mode densities: the density in the volume αV of dielectric material, plus the density in the volume $(1 - \alpha)V$ of vacuum (or, practically speaking, air). This assumption neglects the fact that, for Eq. (5) to be valid for these two contiguous volumes, there should be a conducting wall at the dielectric-vacuum interface. In any event, use of this procedure results in the following equation:

$$\rho_2(f)df = 3K(\alpha)f^2 df \quad , \tag{6}$$

where

$$K(\alpha) = \frac{8\pi V}{3c_0^3} (1 + b\alpha) \tag{7}$$

and

$$b = (\epsilon')^{3/2} - 1 \quad . \tag{8}$$

Comparing Eq. (6) with Eq. (5) we see that the effective dielectric constant is

$$\epsilon'(\alpha) = (1 + b\alpha)^{2/3} \quad . \tag{9}$$

To find the number of modes, $N(\alpha)$, in a lossless cavity, between frequencies f_1 and f_2 one simply integrates Eq. (6), thereby obtaining

$$N(\alpha) = K(\alpha)(f_2^3 - f_1^3) \quad . \tag{10}$$

This equation says that N is a linear function of α[see Eq. (7)], which, in spite of the assumptions used in the derivation, has been verified experimentally for low-loss dielectric fluids such as liquid hydrogen.

In the lossless case, the total number of modes given by Eq. (10) would be observable, except for degeneracies (two or more modes having the same resonant frequencies). This assumes, of course, that we can only distinguish modes on the basis of their resonant frequencies and that we have no way to sample their field patterns. In this "Hohlraum" theory we have no way of computing the number of degeneracies, since their number depends on the details of the boundary conditions. In general, if there are no geometrical symmetries in the structure, there will be no degeneracies. We can try to approximate the effect of degeneracies by multiplying $K(\alpha)$ by a degeneracy factor, $\varkappa_d$. Then, the density of modes becomes

$$\rho_2(f) = 3\varkappa_d K(\alpha) f^2 \quad . \tag{11}$$

In general, $\varkappa_d$ is a function of the frequency interval (f_1, f_2) and of the geometry of the particular cavity of interest; thus, it must be determined empirically. For simplicity, we will assume that $\varkappa_d$ is not a function of α, even though it is likely to exhibit some dependence on this variable.

C. Density of Observable Modes--Lossy Case

In the Bendix system, a probe is coupled into the cavity and the frequency is swept from f_1 to f_2. The modes are counted by noting the peaks in the power absorbed by the cavity--i.e., the dips in the power reflected by the cavity. There are, of course, losses in the cavity walls and in the dielectric material, and a loading on the cavity caused by the external measurement system. These effects combine to produce a finite loaded Q for each mode, which means that the frequency response of each mode is not a sharp delta function, but rather a broadened, Lorentzian function of the form

$$R(f) = \frac{1}{1 + 4Q_L^2\left[\frac{f - f_0}{f_0}\right]^2} \quad , \tag{12}$$

where Q_L is the loaded Q and f_0 is the resonant frequency.

Now consider the overall response of two adjacent modes having the same Q_L, but separated in frequency by an amount ν. The total response is the sum of two responses, each a function having the form of Eq. (12). A study of this total response shows that if

$$\nu \leq \frac{f_0}{2Q_L} \quad , \tag{13}$$

the response has only one peak and it occurs at $f = f_0 + \nu/2$. Here, f_0 is the resonant frequency of the lower-frequency mode. In other words, the two modes cannot be resolved in frequency. On the other hand, if $\nu \geq f_0/2Q_L$, there are two peaks and the two modes can be resolved.

Hence, if all modes have the same loaded Q, there is a critical frequency separation between modes below which no modes can be resolved. Now, the frequency separation between modes is given by the reciprocal of the mode density [Eq. (11)]. Therefore, at the critical frequency, f_c, we have

$$\frac{f_c}{2Q_L} = \frac{1}{3\varkappa_d K(\alpha) f_c^2} \quad , \tag{14}$$

or

$$\bar{f}_c = \left[\frac{2\bar{Q}_L}{3\varkappa_d K(\alpha)}\right]^{1/3} \quad , \tag{15}$$

where $\bar{Q}_L$ is a reference value of the loaded Q. Again, if all the modes have the same Q_L, $\bar{Q}_L$, all the modes are resolvable for frequencies below $\bar{f}_c$, whereas above $\bar{f}_c$ none are resolvable.

We can now define a normalized frequency

$$\eta = f/\bar{f}_c \tag{16}$$

and write an expression for the observable mode density as

$$\rho(\eta) = \rho_\infty(\eta) P(\eta) \quad , \tag{17}$$

where

$$\rho_\infty(\eta) = 2\bar{Q}_L \eta^2 \quad . \tag{18}$$

The function $\rho_\infty(\eta)$ is obtained by rewriting $\rho_2(f)df$ [Eq. (11)] in terms of η and making the identification of $\rho_\infty(\eta)$ with the coefficient of $d\eta$.

The function $P(\eta)$ gives the probability of observing a mode at the normalized frequency η. In the case where all the modes have the same Q_L:

$$P(\eta) = 1 \text{ for } 0 \leq \eta < 1 \tag{19a}$$

and

$$P(\eta) = 0 \text{ for } \eta > 1 \quad . \tag{19b}$$

However, in a practical situation the modes in the frequency band (f_1, f_2) will <u>not</u> all have the same Q_L; that is, there will be a statistical <u>distribution</u> of values for Q_L. Our problem, therefore, is to find a probability function $P(\eta)$ that accurately reflects the properties of this distribution and that reduces to Eq. (19) in the special case when all the Q_L values are the same.

The problem of finding $P(\eta)$ is solved by noting the analogy between the mode-counting problem and the problem of counting the number of electrons in the conduction band of a metal. The latter case is described by Fermi-Dirac statistics,[1] which are based on two major assumptions:

- The particles are indistinguishable
- No more than one particle may occupy a given energy state (there are no degeneracies).

To make the analogy we may read "mode" for "particle" and "frequency" for "energy." The modes in our case are indistinguishable because we only observe them as peaks in the absorption of incident energy and not as configurations of electromagnetic fields. We account for degeneracies by the use of the factor, $\varkappa_d$; that is, degenerate modes are counted as only one mode.

In the case of electrons, the probability that an electron occupies a given energy state, E, is given by the Fermi function:

$$F(E) = \frac{1}{1 + e^{\frac{E - \Phi_F}{kT}}} \quad , \tag{20}$$

where k is Boltzman's constant, T is the absolute temperature, and Φ_E is the Fermi energy (level). At a temperature of absolute zero, electrons occupy all states up to the Fermi level and no states above it. Therefore, Φ_F is analogous to the critical frequency, $\bar{f}_c$, and a temperature of absolute zero corresponds to the case where the values of loaded Q are the same for all modes. Having a distribution of loaded-Q values therefore corresponds to having a finite temperature.

Accordingly, we seek a probability function of the form

$$P(\eta) = \frac{1}{1 + e^{\gamma(\eta-1)}} \quad . \tag{21}$$

The parameter γ must be related to the distribution of Q_L. This is best accomplished by considering the probability density function for Q_L, $p(Q_L)$. We take $p(Q_L)$ to be proportional to the number of modes in (f_1, f_2) with a particular value of loaded Q, divided by the total number of modes in (f_1, f_2). Of course, we normalize $p(Q_L)$ so that

$$\int_0^\infty p(Q_L)dQ_L = 1 \quad . \tag{22}$$

The reader will recall that the quantity $p(Q_L)dQ_L$ is the probability that Q_L' lies between Q_L and $Q_L + dQ_L$. Also, the average or expected value of $(1/Q_L)$, $1/\bar{Q}_L$, that corresponds to the given statistical

distribution is given by

$$1/\bar{Q}_L \equiv \int_0^\infty \left(\frac{1}{Q_L}\right) p(Q_L) dQ_L \quad . \tag{23}$$

It is convenient, then, to work in terms of a normalized Q_L, ξ_L, where

$$\xi_L = Q_L/\bar{Q}_L \quad . \tag{24}$$

We designate the corresponding probability density function for this normalized variable by the symbol $\bar{p}(\xi_L)$.

Note also that for each value of Q_L, there is a corresponding critical frequency, f_c, as given by Eq. (14). Thus, there is also a statistical distribution of critical frequencies. We define a normalized critical frequency, η_c, by the relation

$$\eta_c = f_c/\bar{f}_c \quad , \tag{25}$$

where $\bar{f}_c$ is the "average" critical frequency given by Eq. (15) when $\bar{Q}_L$ is given by Eq. (23). There is also a probability density function for η_c, which we call $q_c(\eta_c)$.

To relate $q_c(\eta_c)$ and $\bar{p}(\xi_L)$ [$\bar{p}(\xi_L)$ is our measured quantity] we note that the probability that ξ_L' is between ξ_L and $\xi_L + d\xi_L$ must be the same as the probability that η_c' is between η_c and $\eta_c + d\eta_c$. Hence,

$$\bar{p}(\xi_L) d\xi_L = q_c(\eta) d\eta_c \quad . \tag{26}$$

From Eq. (15) we find that

$$\eta_c = \xi_L^{1/3} \tag{27a}$$

and

$$d\eta_c = \frac{1}{3}\,\xi_L^{-2/3} d\xi_L \quad . \tag{27b}$$

Substituting these results in Eq. (26) we find that

$$q_c(\eta_c) = 3\,\bar{p}(\eta_c^3)\eta_c^2 \quad . \tag{28}$$

In practice, the probability density function for $Q_L/\bar{Q}_L$, $\bar{p}(\xi_L)$, would have to be determined empirically. Also, it need not be a symmetrical function. However, for the purposes of illustration and, hopefully, as a useful approximation, we will assume that $\bar{p}(\xi_L)$ is a Gaussian function:

$$\bar{p}(\xi_L) = \frac{1}{\sqrt{2\pi}\,\sigma}\, e^{-(\xi_L - 1)^2/2\sigma^2} \quad , \tag{29}$$

where σ is the root-mean-square deviation of ξ_L from unity. From Eq. (28) we have

$$q_c(\eta_c) = \frac{3\eta_c^2}{\sqrt{2\pi}\,\sigma}\, e^{-(\eta_c^3 - 1)^2/2\sigma^2} \quad . \tag{30}$$

As the final step in this development we assume that the following equivalence is valid:

$$1 - P(\eta_c) \equiv \text{prob}\,(\eta_c' < \eta_c) = \int_0^{\eta_c} q_c(\eta_c')\,d\eta_c' \quad , \tag{31}$$

where $P(\eta_c)$ is given by Eq. (21) and $q_c(\eta_c')$ is given by Eq. (30). Equation (31) states that, if the test value of η_c is small (< 1), the

probability that there are smaller values of η_c is small; if the test value of η_c is large (> 1), the probability that there are smaller values of η_c approaches unity. We regard the assumption that this probability equals $1 - P(\eta_c)$ as highly plausible, but we are unable to supply a rigorous proof. The validity of the assumption, therefore, must be tested by experiment. As a result of this assumption, we may write an alternate expression for $q_c(\eta_c)$:

$$q_c(\eta_c) = \frac{d}{d\eta_c}\left[1 - P(\eta_c)\right] \quad , \tag{32}$$

or

$$q_c(\eta_c) = \frac{\gamma}{4\cosh^2\left[\frac{\gamma}{2}(\eta_c - 1)\right]} \quad .$$

We wish Eq. (30) to approximate Eq. (32) as closely as possible. From Eq. (32), note that

$$q_c\left(1 \pm \frac{1}{\gamma}\right) = 0.786\, q_c(1) \quad . \tag{33}$$

If we apply this result to Eq. (30), we find that

$$\gamma \approx \frac{4.32}{\sigma} \quad . \tag{34}$$

Hence, our final result is (assuming a Gaussian distribution for the normalized Q_L values)

$$P(\eta) = \frac{1}{1 + e^{4.32(\eta-1)/\sigma}} \quad . \tag{35}$$

D. Comparison of Models

The model that was developed in the last subsection is compared in this subsection with the model currently used by Bendix. Bendix uses an expression for the probability of observing a mode that is different from Eq. (21). When we write the Bendix expression in terms of normalized frequency we obtain

$$P_B(\eta) = e^{-(2/3)\eta^3} \quad , \tag{36}$$

where it has been assumed that their mode merging parameter β is equal to 0.5. By using Eqs. (17), (18), (35), and (36) we obtain the two corresponding expressions for observed mode density:

SRI:

$$\rho(\eta) = \frac{2\bar{Q}_L \eta^2}{1 + e^{4.32(\eta-1)/\sigma}} \quad , \tag{37a}$$

Bendix:

$$\rho(\eta) = 2\bar{Q}_L \eta^2 e^{-(2/3)\eta^3} \quad . \tag{37b}$$

The behavior of these two functions is compared in Figure 2 for several values of σ. As indicated, the two functions behave dissimilarly except for $\sigma = 1$.

Thus, the Bendix model seems to imply that a broad, but single, distribution of values exists for the loaded Q in every situation, whereas we know that the distribution of loaded Q values can be different in each situation, and a parameter that is a measure of this distribution should enter into the mathematical model. Some adjustment of the Bendix model is possible by varying their mode-merging parameter, β, but any significant deviation of this parameter from a value of 0.5 obscures its physical meaning. Moreover, the Bendix model does not produce the

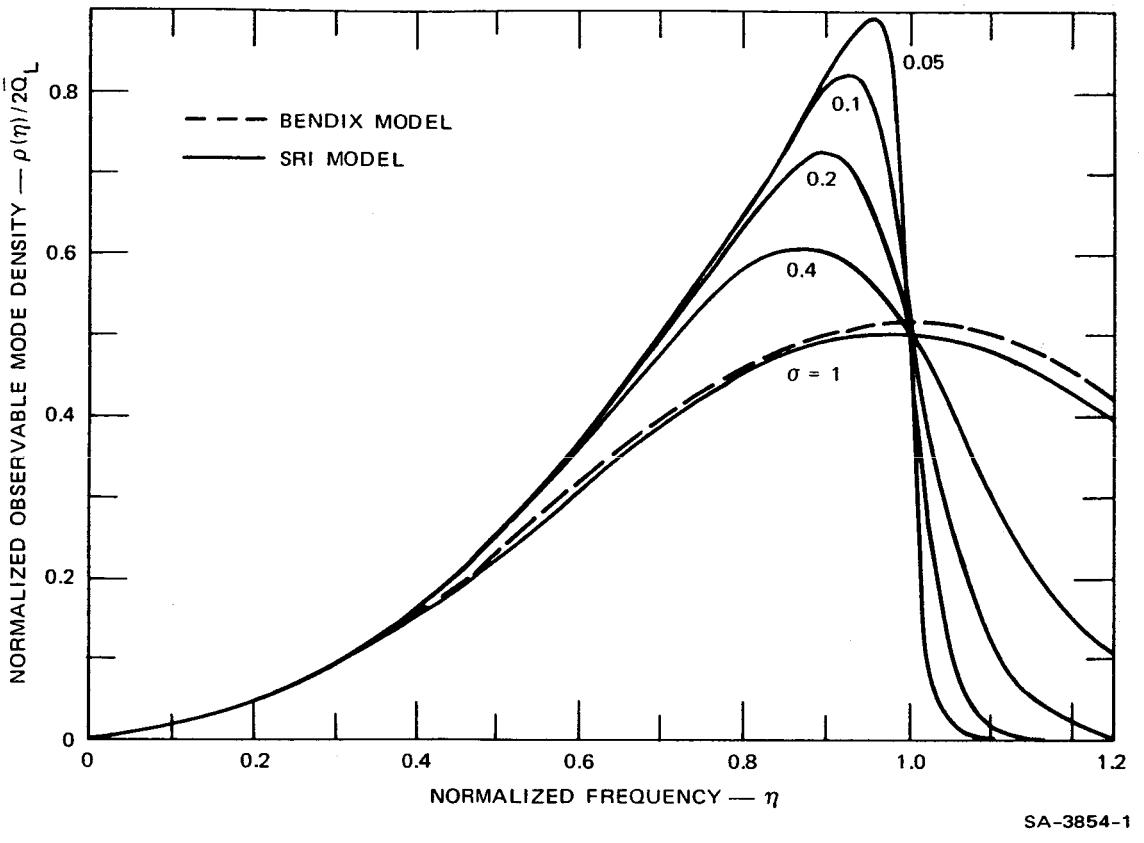

FIGURE 2 COMPARISON OF MATH MODELS

correct results in the limiting case where the loaded Qs of all the modes are the same.

It probably would be impractical, without automated equipment* to measure the loaded Qs of, say, 1,000 modes (or resonances) to determine the statistical parameter σ. On the other hand, σ can be considered as a curve fitting parameter and its approximate value determined from experimental gauging responses that are obtained using a scale-model tank (one might have to assume something other than a Gaussian distribution for the loaded Q to obtain a good fit). However, even though one

*Automated methods for measuring Q are discussed in Appendix B.

uses an approximate value for σ, this new model should be more accurate than the Bendix model unless it turns out that $\sigma \approx 1$. Physically, this situation would correspond to having the loaded Q range from very low values to more than twice the average value. In all fairness, it would not be unreasonable to expect such a distribution to occur occasionally in practice.

For either model, the number of observable modes, $N_o(\alpha)$, in the frequency band (η_1, η_2) is obtained by integrating $\rho(\eta)$ from η_1 to η_2.* Depending on the choice of these limits, one can obtain either a positive or a negative slope for $N_o(\alpha)$. To see this in a qualitative way, we first consider the behavior of $\bar{f}_c(\alpha)$ [see Eq. (15)]. For low-loss dielectrics, $\bar{Q}_L(\alpha)$ does not change significantly as α increases (see discussion in Section E.2), and so the dependence of $\bar{f}_c$ on α is determined by $K(\alpha)$. We see that, as α increases, $K(\alpha)$ increases [see Eq. (7)] and so $\bar{f}_c(\alpha)$ decreases. However, for high-loss dielectrics, $\bar{Q}_L(\alpha)$ decreases rapidly with increasing α, and so in this case $\bar{f}_c(\alpha)$ decreases even more rapidly. The net result of this behavior is that, as α increases from 0 to 1, $\eta_1(\alpha)$ and $\eta_2(\alpha)$ move to the right along the abscissa in Figure 2. The effect on the gauging response, $N_o(\alpha)$, of this relative motion of the end points of the frequency band is illustrated in Figure 3. The curves on the left-hand side of the figure each represent mode density as a function of η in a typical case. The curves on the right-hand side of the figure show the corresponding gauging responses as functions of α.

Figure 3(a) illustrates the case where the end-point frequencies are well below the critical frequencies for both the empty and the full cavities. The cross hatched areas represent the integrals of the mode

---

*Techniques for integrating Eq. (37a) are described in Appendix A.

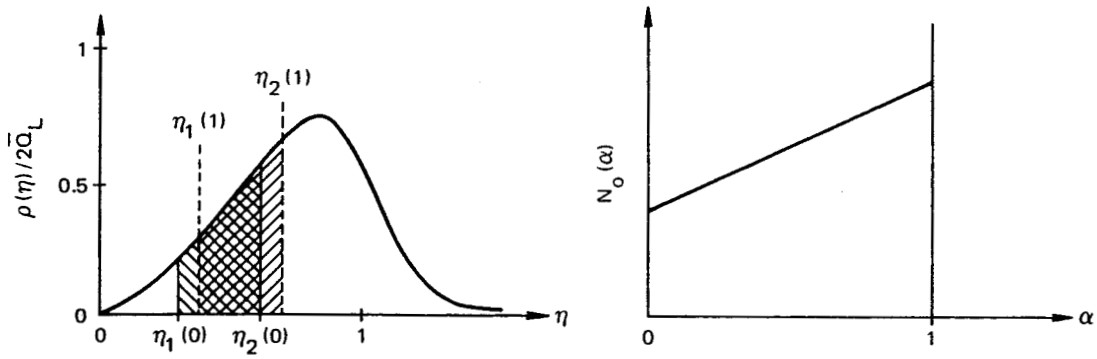

(a) LINEAR RESPONSE — POSITIVE SLOPE

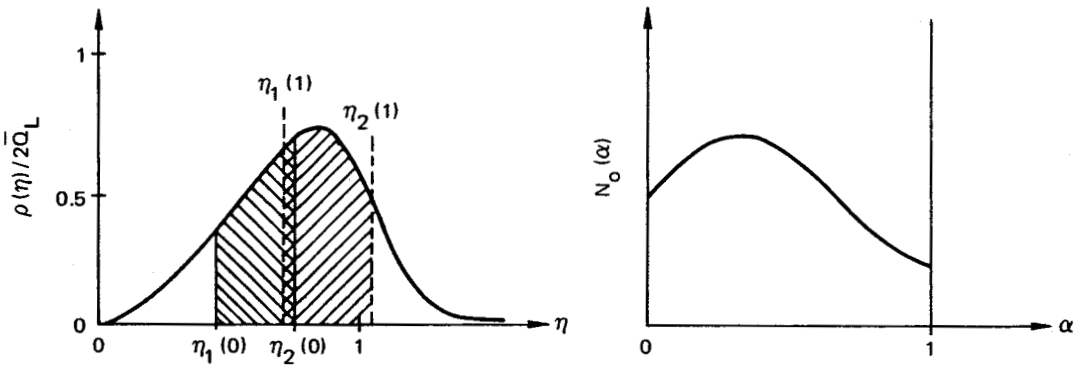

(b) DOUBLE-VALUED RESPONSE — CONTAINS POINT OF ZERO SLOPE

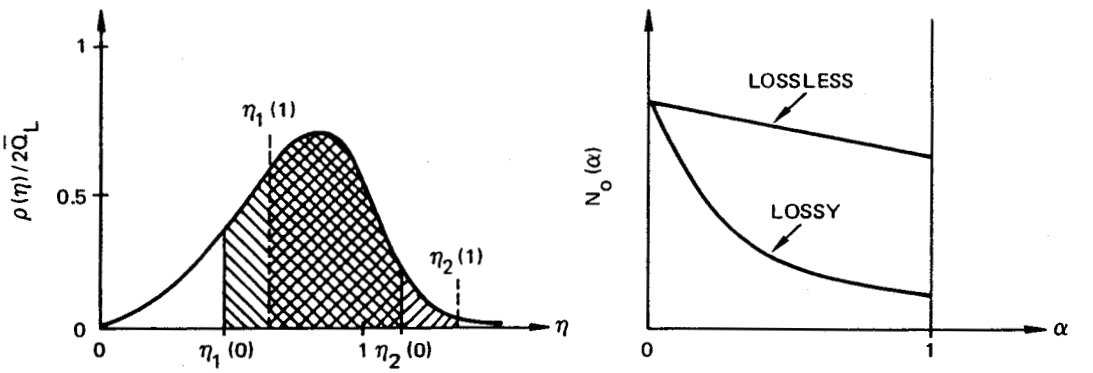

(c) LINEAR AND NONLINEAR RESPONSE — NEGATIVE SLOPE

SA-3854-2

FIGURE 3 ILLUSTRATION OF HOW THE CHOICE OF FREQUENCY RANGE AFFECTS THE GAUGING RESPONSE

density for the empty and full cases. In this regime, mode merging is not significant and the gauging response is a linear function of α; that is, the gauging response is determined by $K(\alpha)$ and not by $\bar{Q}_L(\alpha)$.

Figure 3(b) illustrates the case where both end-point frequencies are below the critical frequency for the empty cavity, but one or both of the end-point frequencies are above the critical frequency for the full cavity. In this case, the gauging response first increases somewhat as does the curve in Figure 3(a), reaches a maximum, and then decreases. The exact shape of this curve depends on how $\bar{Q}_L$ varies with α and, of course, upon σ. This flat, double valued curve is the most unsatisfactory kind of gauging response and cannot be used.

Finally, Figure 3(c) illustrates the case where the lower end-point frequency is well below the critical frequencies for both the empty and the full cavities, whereas the upper end-point frequency is well above the critical frequency in both cases. In this case, we can show that the integral of the mode density is essentially independent of σ, with the result that

$$N_o(\alpha) \approx \frac{2}{3}\bar{Q}_L(\alpha) - K(\alpha)f_1^3 \quad . \tag{38}$$

If $\bar{Q}_L(\alpha)$ = a constant,

$$\frac{dN_o}{d\alpha} \approx -bK(0)f_1^3 \quad . \tag{39}$$

Therefore, a gauging response with a constant negative slope would be observed in practice if the dielectric liquid in the tank were lossless and the frequency limits were chosen according to the above prescription. However, for a lossy dielectric liquid, such as liquid oxygen, the

gauging response is dominated by the behavior of $\bar{Q}_L(\alpha)$ and the gauging response becomes very nonlinear [see Figure 3(c)]. We note, however, that the slope of the gauging response for a lossy dielectric typically is much greater than for a lossless dielectric. Thus, having a lossy dielectric should improve the measurement precision, but only if the dynamic range of the measurement system is large enough to avoid miscounting the modes when the filling of the cavity with lossy dielectric reduces the measurement sensitivity.

This sort of general behavior of gauging response according to the choice of end-point frequencies was also noted by Bendix. For example, for liquid oxygen they stated that the optimum choice would be f_1 as the frequency where the mode density for the filled tank was at a maximum, and f_2 as the frequency where the full-tank mode density went to zero. This choice is similar to the case shown in Figure 3(c), but would result in an even more rapidly decreasing gauging response than that shown in the figure. This choice can probably be considered to be optimum for lossy dielectric fluids (from the point of view of maximum measurement precision), provided that the coupling to the filled cavity is not so weak that modes become undetectable. On the other hand, the critical frequency for low-loss dielectric fluids may be so high that a practical choice of frequency band leads to the linear response shown in Figure 3(a). In this case, the choice of an optimum band might be based on the availability of components or on the minimization of equipment complexity and cost.

E. Accuracy and Limitations of the Model

Based on our previous discussions, we can identify four problem areas that will limit the accuracy of the math model:

(1) Breakdown of the Hohlraum assumption for nearly empty or nearly full cavities.

(2) Practical difficulties in accurately determining $\bar{Q}_L(\alpha)$ and σ.

(3) Degeneracies and spurious modes.

(4) Variations in coupling.

A discussion of each of these points follows.

1. Breakdown of the Hohlraum Assumption

The theory assumes that the total density of modes in the cavity is equal to the sum of the density of modes in the dielectric material and the density of modes in the vacuum. However, if only a small amount of dielectric material is in the cavity, the subvolume of dielectric material is not large compared with an electromagnetic wavelength, which contradicts our basic Hohlraum assumption. By comparing an exact analysis of a simple rectangular cavity that is partially filled with dielectric material with the results obtained from our theory, we find that the true value for the density of modes in a small volume of dielectric material is always slightly less than the value predicted by the Hohlraum theory. This effect causes the theoretical gauging response to overestimate the true mode count over the whole range of α. This means that, for a given value of mode count, the theory underestimates the true value of α. In the example studied, the error in α was approximately 0.01, independent of α. The corresponding percentage error as a function of α is shown in Figure 4. Obviously, for small values of α the percentage error in α becomes very large. In principle, this error in prediction could be significantly reduced for all but the very smallest values of α if an appropriate effective volume and dielectric constant were used in the theory. However, determination of these effective values would require that some measurements be made on the cavity for various values of α, which might not be worth the trouble.

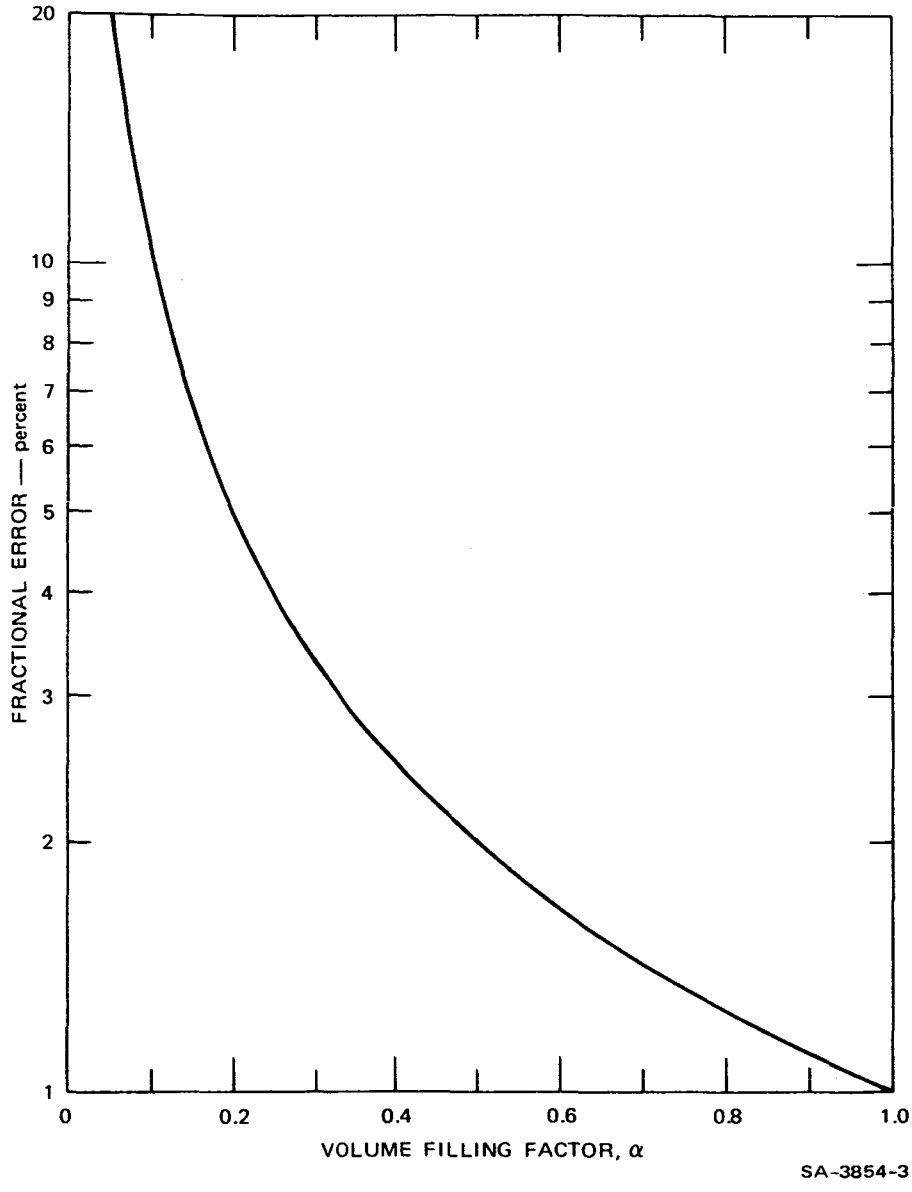

FIGURE 4 PERCENTAGE ERROR IN THE GAUGED VALUE OF α (assuming $\Delta\alpha = 0.01$)

A similar breakdown in the Hohlraum assumption occurs when the cavity is nearly full. In this case the subvolume of vacuum (i.e, air) is not large compared with an electromagnetic wavelength. In addition, the situation can arise where most of the modal energy resides in the dielectric material and the modes in the vacuum are "cut off," that is, their fields decay exponentially with distance. This results in the mode density in the vacuum being effectively reduced even further.

However, since the total mode density in the "nearly full" case is determined primarily by the mode density in the dielectric material, which is larger than that for the same size air space in the "nearly empty" case, we would expect the predictive errors caused by uncertainties in the vacuum mode density to be relatively small.

2. Determination of $\bar{Q}_L(\alpha)$

The symbol $\bar{Q}_L(\alpha)$ represents the average value of Q_L for a particular value of α. Since the determination of the average value requires a large number of measurements, it is only practical to make the measurements for one value of α, say $\alpha = 0$. Therefore, we need a relationship that will allow us to predict $\bar{Q}_L$ for other values of α.

In general, the loaded Q of a mode having a resonant radian frequency of ω_0 is given by the relation

$$\frac{1}{Q_L} = \frac{\Sigma P_\ell}{2\omega_0 W_E} \quad , \tag{40}$$

where ΣP_ℓ is the sum of all the powers dissipated in the cavity or escaping from the cavity, and W_E is the total energy stored in the electric field. Equation (40) is usually written in the form

$$\frac{1}{Q_L} = \frac{1}{Q_e} + \frac{1}{Q_u} \tag{41a}$$

or

$$\frac{1}{Q_L} = \frac{1 + \beta}{Q_u} \quad . \tag{41b}$$

Here, Q_u is the "unloaded" Q that is related to the power that is dissipated inside the cavity (wall and dielectric losses), and Q_e is

the "external" Q that is related to the power dissipated in the external measuring system. Alternatively, the coupling parameter β may be used instead of Q_e. Note that Q_u can be decomposed still further as follows:

$$\frac{1}{Q_u} = \frac{1}{Q_0} + \frac{1}{Q_d} \tag{42}$$

where Q_0 is determined by the power dissipated in the walls and Q_d by the power dissipated in the dielectric material inside the cavity. The quantity Q_d is called the "dielectric Q." We need to consider these various Q factors in turn to see how they might vary with α.

First consider Q_0. It is well known from quite general considerations that for any mode

$$Q_0(\alpha) = B_0[f_0(\alpha)]^{\frac{1}{2}} \quad , \tag{43}$$

where $f_0(\alpha)$ is the resonant frequency for a particular value of α and B_0 is a proportionality constant that is independent of α. Thus, each mode with a different resonant frequency has a different Q_0. Now, as the cavity is filled with dielectric material, a given mode at frequency f_0 will be replaced by another mode that originally had a higher resonant frequency. Therefore, the value of Q_0 associated with a particular frequency f_0 would not depend on α except for the fact that the proportionality factor B_0 is, in general, different for each mode because of the geometrical effects associated with the different field configurations of each mode. However, because there are many modes involved, it is reasonable to assume that the average value of $(1/Q_0)$ over the band (f_1, f_2), $1/\bar{Q}_0$, does not depend on α--that is, we expect an increase in Q_0 at one frequency to be compensated by a decrease in Q_0 at another frequency.

Similarly, for the external Q, Q_e, it can be shown that

$$Q_e(\alpha) = B_e f_0(\alpha) \quad , \tag{44}$$

where B_e is also a proportionality constant. Hence, we may use the same reasoning about $Q_e(\alpha)$ as we did for $Q_0(\alpha)$, and thus we assume that the average value of $(1/Q_e)$, $1/\bar{Q}_e$, does not depend on α.

The dielectric Q, Q_d, is different. Suppose the dielectric material in the cavity has a complex relative dielectric constant of $\epsilon' - j\epsilon''$. Then a general relation for the dielectric Q of a partially filled cavity is given by[2]

$$\frac{1}{Q_d(\alpha)} = \frac{1}{Q_d(1)} \frac{W_{\epsilon'}}{W_E} \equiv \frac{1}{Q_d(1)} \Psi(\alpha) \quad , \tag{45}$$

where $W_{\epsilon'}$ is the electric energy stored in the dielectric material, W_E is the total stored electric energy, and

$$\frac{1}{Q_d(\alpha)} = \frac{\epsilon''}{\epsilon'} \quad . \tag{46}$$

In general, the filling factor, $\Psi(\alpha)$, can be written as

$$\Psi(\alpha) = \frac{\epsilon' \int_{\alpha V} |\vec{E}|^2 dV}{\epsilon' \int_{\alpha V} |\vec{E}|^2 dV + \int_{(1-\alpha)V} |\vec{E}|^2 dV} \quad . \tag{47}$$

If, for a large cavity, we assume

$$\int_{\alpha V} |\vec{E}|^2 dV \approx \Delta V \, E_{AV}^2 \quad , \tag{48}$$

where ΔV is any subvolume in V, then we obtain

$$\Psi(\alpha) \approx \frac{\alpha\epsilon'}{1 + \alpha(\epsilon' - 1)} \quad . \tag{49}$$

Analysis of a simple cylindrical cavity partially filled with dielectric material shows this to be a good approximation. In this approximation, $Q_d(\alpha)$ is the same for every mode and so the average value of $1/Q_d(\alpha)$ is the same as $1/Q_d(\alpha)$.

As a result of all the assumptions discussed above, we can now use Eqs. (41a), (42), (45), and (49) to write the following expression for the average value of the reciprocal loaded Q:

$$\frac{1}{\bar{Q}_L(\alpha)} = \frac{1}{\bar{Q}_e} + \frac{1}{\bar{Q}_0} + \frac{1}{Q_d(1)} \frac{\alpha\epsilon'}{1 + \alpha(\epsilon' - 1)} \quad . \tag{50}$$

From this equation,* we can determine one of the three quantities $1/\bar{Q}_L(0)$, $1/\bar{Q}_e$, and $1/\bar{Q}_0$ if the other two are known. To determine the average reciprocal Qs, we must first measure the loaded Q of all the modes in the empty cavity for the frequency band (f_1, f_2) and then find the probability density function $p(Q_L)$. Use of Eq. (23) then gives $1/\bar{Q}_L(0)$. Similarly, measurement of Q_0 (or Q_e) for all the modes and subsequent use of Eq. (23) with Q_L replaced by Q_0 (or Q_e) gives $1/\bar{Q}_0$ (or $1/\bar{Q}_e$).

The point is that to make such a large number of Q measurements may or may not be practical, depending on the equipment available. One may be forced to limit the number of Q measurements that he makes and

---

*Note that this equation differs slightly from the one used by Bendix--i.e., Eq. (2.31) in Ref. 5.

thereby increase the uncertainty in $\bar{Q}_L(\alpha)$. Since $N_o(\alpha)$ depends on $\bar{Q}_L(\alpha)$, this uncertainty in $\bar{Q}_L(\alpha)$ will introduce an error in the gauging response. The magnitude of the error in gauging response will depend on the magnitude of $\bar{Q}_L$ and the choice of frequency limits.

Similar comments apply to the determination of σ, since $p(Q_L)$ is also required. However, $N_o(\alpha)$ is not as sensitive in general to errors in σ as it is to errors in $\bar{Q}_L(\alpha)$. Alternatively, one could choose, as we have mentioned, to determine σ by considering it as a curve-fitting parameter and selecting its value to provide the best fit between the theoretical and measured gauging responses.

3. Degeneracies and Spurious Modes

We have already mentioned the problem of degeneracies: two or more modes get counted as one mode and the effective mode density is less than that predicted by theory. We attempt to account for this effect by multiplying $K(\alpha)$ by a factor $\varkappa_d$, which, for simplicity, we assume is independent of α. The use of $\varkappa_d$ is equivalent to the use by Bendix of an "effective volume." The implication of this is that the same percentage of modes will be lost, regardless of whether the total mode count is high or low.

The validity of the assumption that $\varkappa_d$ does not depend on α is uncertain. Intuitively, we can visualize the introduction of dielectric material into the cavity as breaking some degeneracies, while causing other previously nondegenerate modes to coalesce. An analysis of a partially filled cavity having a simple shape might indicate the degree of validity of this approach, but there was not enough time to carry out such an analysis in this study.

The parameter $\varkappa_d$ can be determined empirically from a measurement of the empty-cavity mode count. This determination is most easily

accomplished when the frequency band is chosen in correspondence with Figure 2(a) because

$$N_o(0) = \varkappa_d K(0)[f_2^3 - f_1^3] \quad . \tag{51}$$

This assumes that no modes are so badly undercoupled that they cannot be detected. If this is not true, $\varkappa_d$ cannot be measured readily unless the number of undetectable modes is known.

One must be concerned with spurious resonances if there are objects in the cavity that are sufficiently decoupled from the cavity so that they can support their own high-Q resonant modes. For example, such an object might be a ladder in the fuel tank. If such spurious modes are detected, it is not a fundamental problem because it should always be possible to design any extraneous objects in the cavity so that the Q of any self-resonance is much lower than the Q of the cavity modes, without damping the cavity modes.

4. Variations in Coupling

One reason that variations in coupling occur is because the interaction of a mode with the coupling element (probe, loop, and the like) depends very much on the electromagnetic field configuration of that mode. The fact that the cavity is large compared with a wavelength does not change the situation. By the same token, the Hohlraum theory cannot predict this effect--that is, the loss of observable modes through insufficient coupling. The best we can do is to multiply N_o by a factor $\varkappa_s$ to try to take account of this reduction in mode count if it occurs. Like $\varkappa_d$, $\varkappa_s$ must be determined empirically, and it is difficult to measure if degeneracies also occur.

In practice, it would be best to avoid having insufficient mode coupling, if possible. One approach for accomplishing this is to use a "space diversity" probe like that currently being used by Bendix. In this way, modes that are not detected by one probe are likely to be detected by another, having a different location and/or orientation.

A variation in coupling that occurs for every mode and that is implicitly contained in theory is the one that occurs when a lossy dielectric material begins to fill the cavity. This variation in coupling is described by the average coupling parameter, $\bar{\beta}$. The following equation for $\bar{\beta}$ is obtained from Eqs. (41b), (42), and (50):

$$\bar{\beta}(\alpha) = \frac{\bar{Q}_0/\bar{Q}_e}{1 + \bar{Q}_0 \Psi(\alpha)/Q_d(1)} \quad . \tag{52}$$

If we define

$$\bar{\beta}_e \equiv \bar{Q}_0/\bar{Q}_e \tag{53a}$$

and

$$\bar{\beta}_d \equiv \bar{Q}_0/Q_d(1) \quad , \tag{53b}$$

Eq. (52) becomes

$$\bar{\beta}(\alpha) = \frac{\bar{\beta}_e}{1 + \bar{\beta}_d \Psi(\alpha)} \quad . \tag{54}$$

A plot of $\bar{\beta}/\bar{\beta}_e$ as a function of α is shown in Figure 5 for several values of $\bar{\beta}_d$. We see that, for finite values of $\bar{\beta}_d$, the coupling to the cavity decreases as α increases. For liquid oxygen, a typical value for $\bar{\beta}_d$ is a number greater than 10. Therefore, in this case we can

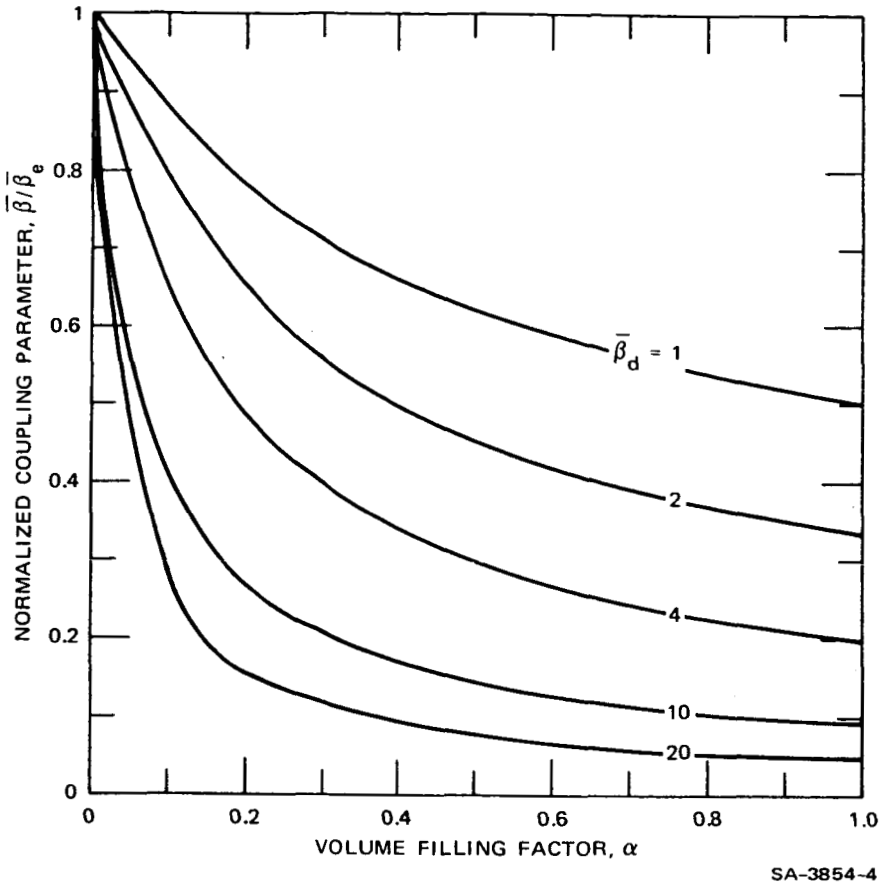

FIGURE 5 VARIATION OF COUPLING FACTOR WITH VOLUME FILLING FACTOR

expect an order of magnitude reduction in the average coupling as the cavity is filled. Hence, the coupling factor for the empty cavity and the sensitivity of the detection system should be large enough so that modes are not undetected when the cavity is filled.

F. Comparison of Theory and Experiment

Now that we have discussed the theoretical math model in detail, it is of interest to compare the theory with some experimental data that have been obtained by Bendix. The most complete set of data available to us was obtained for the Bendix cryogenic tank.[3,4] Unfortunately, there were not enough data pertaining to Q to allow us to determine $p(Q_L)$. Therefore, we used simple arithmetic averaging of the available data to estimate that

$$\bar{Q}_0 = 13,000$$

and

$$\bar{\beta}_e = 0.24 \quad .$$

The other parameters given for the system were

$$f_1 = 1.03 \text{ GHz},$$

$$f_2 = 2.0 \text{ GHz},$$

and

$$V = 0.8876 \text{ m}^3 \quad .$$

Finally, the corresponding material parameters were:

Liquid hydrogen:

$$\epsilon' = 1.2$$

$$\epsilon'' = 10^{-7}$$

$$b = 0.31$$

$$\bar{\beta}_d = 1.1 \times 10^{-3}$$

Liquid oxygen:

$$\epsilon' = 1.5$$

$$\epsilon'' = 0.00136$$

$$b = 0.84$$

$$\bar{\beta}_d = 11.8$$

From the given volume and the known velocity of light, we find that

$$K(0) = \frac{8\pi V}{3c_0^3} = 2.75 \times 10^{-25} \quad . \qquad (55)$$

First, consider the experimental data for liquid hydrogen shown in Figure 6. In this case, we calculate that $\bar{f}_c(0) = 3.2$ GHz and $\bar{f}_c(1) = 2.9$ GHz. Hence, $\eta_1 \approx 0.33$ and $\eta_2 \approx 0.67$, which means that the gauging response should be linear if $\sigma \lesssim 0.4$. We see that the measured gauging response shown in Figure 6 is indeed linear. We note that $N_o(0) = 1450$, so from Eq. (51), we find that

$$\varkappa_d = 0.764 \quad , \tag{56}$$

where we assume that no modes have been lost because of insufficient coupling. Now, because our frequency band is well below the critical frequency, we can use Eq. (10), multiplied by $\varkappa_d$, to calculate the gauging response. This result is also shown in Figure 6. Since the slope of this curve does not match that of the measured curve,

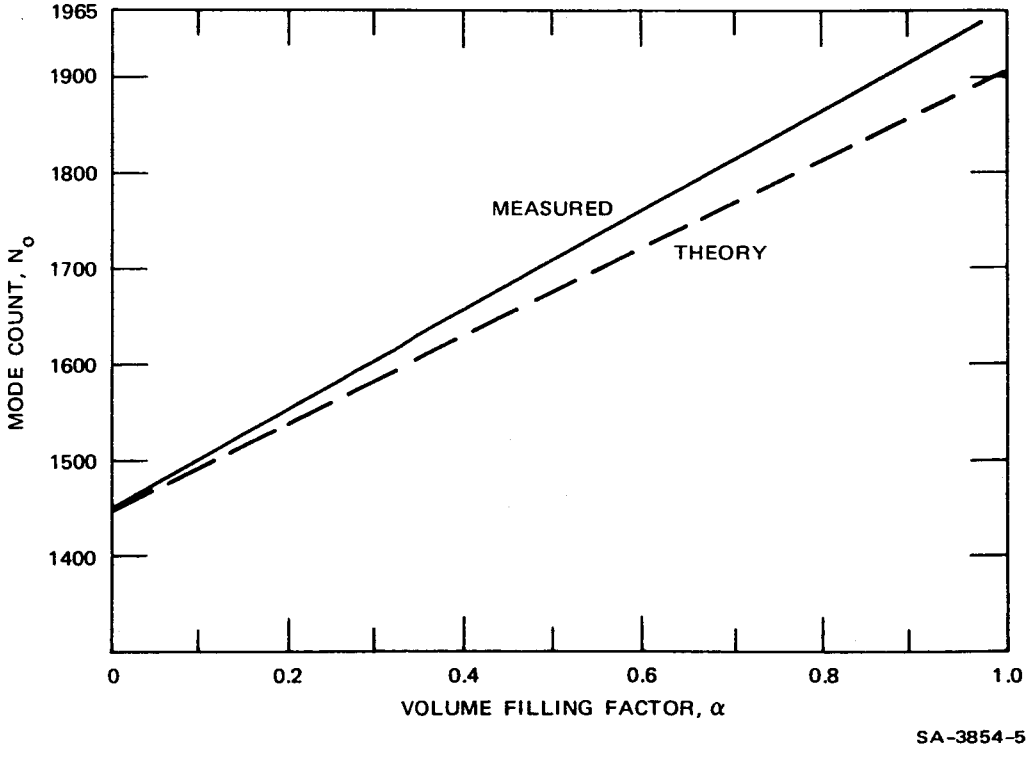

FIGURE 6 COMPARISON OF MEASURED AND THEORETICAL GAUGING RESPONSES FOR BENDIX CRYOGENIC TANK AND LIQUID HYDROGEN

we must conclude that the value of the dielectric constant used in the theory was not the same as that of the actual fluid.

The experimental data obtained for liquid oxygen in the same cryogenic tank are shown in Figure 7 as the heavy solid curve. We immediately

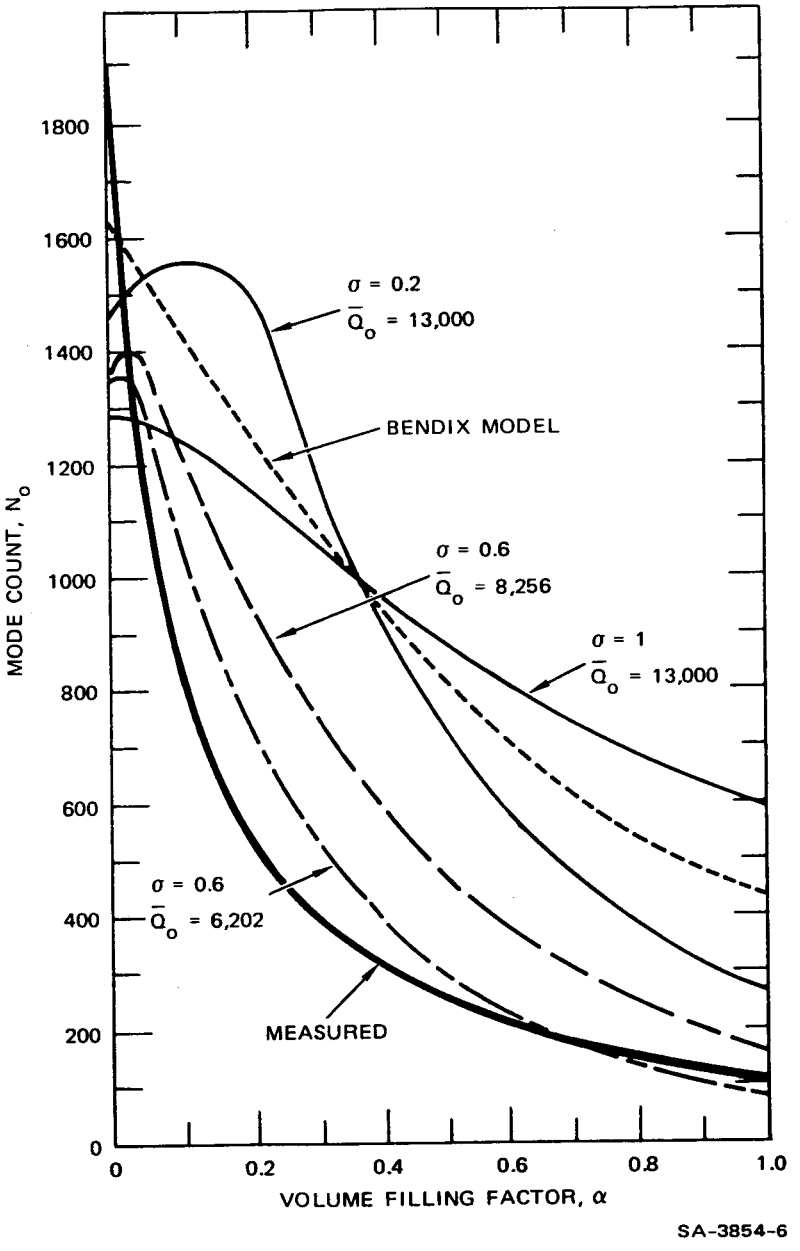

FIGURE 7 COMPARISON OF MEASURED AND THEORETICAL GAUGING RESPONSES FOR BENDIX CRYOGENIC TANK AND LIQUID OXYGEN

note a discrepancy which we cannot explain: $N_o(0)$ in this case is different from the value obtained in the liquid-hydrogen case. Apparently, this means that something in the system changed between measurements.

To complete our theoretical comparison, we have no choice but to use the value of κ_d obtained from the liquid-hydrogen data--that is, Eq. (56). The light solid curves in Figure 7 show the corresponding responses that we calculate for two different values of σ. For comparison, the dashed curve shows the theoretical results computed by Bendix using their math model. The fact that their curve does not agree with our $\sigma = 1$ curve indicates that they must have used different values for the parameters.

None of these theoretical curves agree well with the measured curve. If we compute the values for the critical frequency, we find that

$$\bar{f}_c(0) = 3.2 \text{ GHz},$$

which means that

$$\eta_1(0) = 0.32$$

and

$$\eta_2(0) = 0.62 \quad .$$

Similarly,

$$\bar{f}_c(1) = 1.2 \text{ GHz},$$

which means that

$$\eta_1(1) = 0.86$$

and

$$\eta_2(1) = 1.67 \quad .$$

Thus, we see that the case shown in Figure 3(b) is applicable. Therefore, to make our theoretical curve come closer to the measured curve, we must assume a lower value for the loaded Q so that the critical frequency will be lower [see Eq. (15)]. The broken curves in Figure 7 show two examples of the results that are obtained when lower $\bar{Q}_0$-values (resulting in lower $\bar{Q}_L$) are assumed. As indicated in the figure, the assumption of a fairly low $\bar{Q}_0$ results in much better agreement between theory and experiment, provided that the parameter σ is also varied. It appears that further variation of the parameters in the model might provide better agreement.

Unfortunately, this example does not prove the validity of the model. The model seems to predict the right kind of general behavior for the gauging response, provided the proper parameter values are used. Although we have not shown that it is possible to measure these parameters, we feel that it should be possible to do so if enough Q measurements are made, and if the system is stable so that the data are repeatable.

III GENERAL MICROWAVE RESONATOR AND SYSTEM CONSIDERATIONS

A. Resonator Coupling

After extensive experimentation, Bendix has adopted--as its definitive method for coupling to the microwave resonances of the fuel tank--a composite probe comprising four elements, each of which is best described as a short E-field probe. (Describing them as "monopoles" is not recommended because the ground plane for each "whip" is not clearly defined and the length of each "whip" is not intended to be quarter-wave resonant.) The orientations of the four elements are "randomized" (within reason, insofar as mechanical convenience has allowed) and the average spatial separation is about one-fourth the mean operating wavelength (see Figure 5-10 of Reference 4).

Since no theory could adequately comprehend all the factors involved, it can be accepted that this arrangement is adequate, and perhaps optimum, if empirical studies (i.e., experimentation with different orientations, separations, and numbers of probe elements) have not produced a coupler giving better results for the particular tank, dielectric fluid, and frequency range of interest. "Better results" may be interpreted simply as indicating an observed mode count that is higher, and presumably closer to the theoretical; no coupler can introduce counts that should not be there, but a less than ideal coupler can allow modes to go uncounted. Because this probe samples different directions in space, and because it is assumed that the cavity dimensions are very much larger than a wavelength, the position of the probe in the cavity should not matter.

The elements of the Bendix multiprobe coupler are not fed in parallel. Rather, they are fed singly, in time sequence, with the resultant four sets of mode detection data processed appropriately. "Appropriately" here means that at any one frequency a mode should be counted even if it is "seen" by only one of the probes. At the same time, a mode should be counted no more than once even when it is "seen" by all four probes. The processing used should be made relevant to these criteria, rather than considered as merely "summing" and "averaging." For example, suppose a certain frequency interval contained M + P resonant modes, where M modes coupled to all four probes and P modes coupled to only one probe. "Summing" and "averaging" the four output counts (as suggested on Page 55 of Reference 4) would incorrectly yield M + P/4 modes. Summing and averaging the video waveform prior to counting, however, could give a correct result.

One may ask if it would not be simpler and cheaper to connect the diversity probe elements in parallel rather than switch them sequentially. As a general principle, yes, but as a practical possibility, no. Over the wide frequency range required, the finite lengths of transmission line between elements would lead to wild fluctuations of the overall input impedance, and at some frequencies one or two of the probes might be fed no power at all. The phases of the excitation of the several probes could also possibly be such as to produce zero net coupling to some resonant mode in the tank, whereas this is unlikely with only one probe fed at a time, and the remaining probes isolated at that time. The techniques currently in use (assuming correct mode-pattern processing) therefore appear justifiable.

The coupling to a resonant mode in a cavity can either be under, over, or critically coupled, as is well known. In examining the frequency swept reflected signal from the coupling probe, the "suck out" (or "dip") will be deepest at critical coupling. With under coupling,

the "suck out" will be less deep, but its width will be narrower. With the present means of processing the video waveform to detect resonances, the increased narrowness of the "suck out" might increase its chances of detection about as much as the decreased depth may have lessened the chances. It is apparent, therefore, since the tightness of coupling must vary widely from mode to mode, that the best approach is to keep the probes sufficiently short so that the under-coupling condition will predominate. Critical coupling would then also be observed for some modes, but over-coupling only rarely. With over-coupling, the "suck outs" are both wider and shallower, and the chances of detection doubly worsened.

It is of interest to note the technique* used by microwave oven manufacturers to couple into their over-moded resonators. Their coupler (usually a waveguide iris only slightly smaller than the feed waveguide with which it is combined) is pre-adjusted to be matched into free space. This coupler is then found to be about optimum over a wide range of oven loadings (with foodstuffs, plastics, and so on). This result is consistent with the picture that the Q values are quite low and that the input energy makes relatively few "bounces" around the chamber before it is absorbed. The locations of the feed, the stirrer (which is often designed remarkably like the revolving mirrors in a dance hall), and the material to be heated are arrived at by assuming the RF energy arrives along a straight line path and "bounces off" the conducting surfaces for just a few passes. In this case (with tight coupling and low Q_L), it is evident that a multiplicity of modes is being excited (it takes many modes to synthesize a plane wave) even though the frequency is singular, and even when the "stirrer" is not

*Gerling Moore, Inc., private communication.

moving. In other words, we may say that many modes have "merged." A comparable situation in the fuel tank gauging system would therefore be highly undesirable. This discussion, hopefully, contrasts the "microwave oven" and "fuel tank" situations. In particular, the idea of an antenna radiating into free space and "illuminating" (well or badly) the interior of the fuel tank is inapplicable.

B. Resonator Geometry

The basic premise of a cavity with very large dimensions compared with a wavelength leads to the conclusion that the total mode count over a given frequency range depends only on the volume enclosed and not on the specific dimensions of the cavity or its shape. Perturbations, except for the effects of losses which may make a mode more difficult to count in the experimental situation, should therefore only alter the total mode count in proportion to the perturbing volume. This means that the insertion of struts, ladders, probe supports, and the like, into the cavity should only result in a mode count that is appropriate to the final volume, though care should be excercised to avoid the introduction of lossy materials, resistive contacts, and so on. One should also be aware of the possibility that the insertions may create partially shielded "subvolumes" with dimensions comparable to the wavelength. Such subvolumes will reduce the mode count because their effective electrical volumes will be less than their physical volumes by an amount which is difficult to predict.

It is possible that a perturbation of the cavity (e.g., a strut or ladder) might support its own resonance, or series of resonances, in the frequency range of interest. The dependency between total mode count and dielectric filling might then be thrown off. In the case of the fuel tank, it appears inconceivable that such resonances (e.g., from

a slot of critical length) might be so "screened off" from the tank volume that a narrow "suck out" would appear in the frequency swept video waveform--that is, only in the most unlikely case of a high-Q parasitic resonator being but weakly coupled to the fuel tank volume would the dip appear in the trace. An example of such a parasitic resonator deliberately contrived to illustrate the effect (and the unlikelihood of its occurring by accident) would be a small, hollow, metal volume interconnecting with the fuel tank by means of only a small hole.

For cavities with symmetry about one or more axes, "degeneracies" indeed occur, and the modes that can be counted are fewer than the number that actually exist. In the case of a cavity whose dimensions are only a few times larger than a wavelength, distorting a wall or introducing some other symmetry destroying perturbation does effectively "break up" the degeneracies and increase the total mode count.

In the case of cavities with dimensions very large compared with a wavelength, however, the situation is quite different. The mode density is very high and the spacing between most modes is small. Any perturbation capable of resolving a degeneracy by frequency shifting one of two merged modes enough for it to be countable could, with equal likelihood, shift it into superposition with some other nearby mode. There is no choice but to conclude that it is pointless to even consider solving the "degeneracy problem" through deliberate introduction of deformations or perturbations into the truly large cavity. An asymmetrical location or orientation of the coupling probe could, however, have merit, but only as an additional degree of diversity for a diversity type probe.

When <u>all</u> cavity dimensions are large compared with the wavelength, the unloaded Q, $Q_u = Q_0$ (assuming ideal lossless dielectric filling)

should not be enormously affected by whether the cavity is reentrant or not. However, the Q_0 for the reentrant case should be somewhat lower than for the nonreentrant case, since lower volume-to-surface ratios will be encountered (locally or globally). Experimental observations indicating a significantly reduced Q_0 in the reentrant case might well be caused by artifacts such as extra resistance in a welded joint.

The effects of intermittent contacts and excessive resistance in a welded or clamped joint can be considerable when the Q_0 in the absence of these effects can potentially be quite high. The basic premise of a cavity all of whose dimensions are very large compared with wavelength leads to the conclusion that changes of cavity shape or position of internal objects that do not alter the net volume cannot affect the mode count. Therefore, rigidity (of a probe and the like) should not have to be maintained, in principle. Any detrimental effects caused by relative motion between parts that are observed would probably be traceable to the effects of intermittent or lossy contacts near a joint.

Threaded joints are notoriously lossy and unreliable at microwave frequencies. Even when the fit appears tight, contacts may only be occurring at a few well separated points. Threaded joints should categorically be avoided unless the circumference of one turn of the thread is a very small fraction of the smallest wavelength. When a portion of a cavity wall must be demountable, a "biting edge" contact design--with pressure applied at a multiplicity of points--is recommended.

C. Fuel Movement

The most fundamental assumption on which the chosen fuel gauging method has been based is that the total number of modes of resonance possible (in a given frequency range) is independent of the location or

distribution of the dielectric material that may partially fill the cavity. This assumption becomes justified when all cavity dimensions are large compared with a wavelength; the larger the ratio of cavity dimensions to a wavelength the greater the accuracy and consistency of the results based on this assumption. For the large ratios applicable to the system being studied, the variation in the total number of modes possible, occurring as a given amount of fluid changes shape or position in the tank, should be very small.

However, if the movement of the fuel could somehow affect the coupling between the probe(s) and the cavity, the observed mode count might change whenever the coupling became too weak or too strong. For example, one might visualize the case of a substantial quantity (say, of the order of half the tank volume) of high dielectric constant, low-loss fluid moving to the tank end furthest from the coupling probe. The concentration of stored energy in the dielectric could well make Q_e much higher (weaker coupling) than when the fluid is closer to the probe.

A more likely effect is the change in the electrical properties of the probe(s) that immersion in a fluid of arbitrary dielectric constant and loss factor might produce. Either an increase or a decrease in the ability to count all the cavity modes might then occur as the fluid moved toward the probe(s).

In conclusion, one is compelled merely to recommend that the coupling probe(s) be designed and adjusted so that the highest possible mode count (fewest modes lost because of inadequate coupling) is obtained with a given filling of fuel (or simulated fuel) located in the worst possible (empirically determined) position with regard to the coupling effectiveness of the probe(s).

D. Temperature Effects

The possible effects of changes in temperature on the fuel gauging system should be divided into two types: (1) effects that change the total number of modes that can exist in the cavity, and (b) effects that affect the observability of the existing modes.

In category (a) we have the following possible effects:

(1) Changes in the volume of the tank because of temperature-induced expansions or contractions of the metal walls.

(2) Warping or changes in the shape of the tank.

(3) Changes in the dielectric constant of the dielectric fluid in the tank.

(4) Changes in the dielectric properties of the foam insulation sometimes used as a liner within the cavity, between the fluid and the metal tank (and of any other dielectric objects that might be in the tank).

The changes in the number of existing modes produced by effects (1), (3), and (4) should all be predictable, and can be taken into account when necessary. This may require the use of one or more temperature sensors and a compilation of the several temperature coefficients involved. The change caused by effect (2) should be nil, as discussed in Section III-B.

The possible effects to be enumerated under category (b) are:

(1) Changes in the RF loss in the cavity walls or in the dielectric material within the cavity.

(2) Changes in the coupling to the cavity.

Both effects (1) and (2) alter the loaded Q of the cavity, and hence they affect the observability of modes because they affect the depth

of a "suck out" and the degree to which the modes merge. If the loaded Q is dominated by one source of loss--for example, by the loss in the dielectric fluid--then changes in wall losses or coupling are not likely to have a significant effect. On the other hand, for low-loss fluids, effects caused by changes in wall losses or in coupling are more likely to be noticeable. Note, however, that although the coupling might be affected if the coupling probe elements employ dielectric materials or metals whose properties change significantly with temperature, it is hard to conceive that such effects would be appreciable.

E. Data Processing

Consider the representative fragment of "detected mode pattern" of Figure 8, as supplied by Bendix (Figure 4-10, Reference 5). In the frequency interval A (and assuming the modes to be counted are the upward pointing spikes), four modes would be counted by the Bendix signal-processing methods. These four spikes have roughly the same width, which is about as narrow as any of the modes in the entire mode pattern. However, it is possible to visualize that these four modes

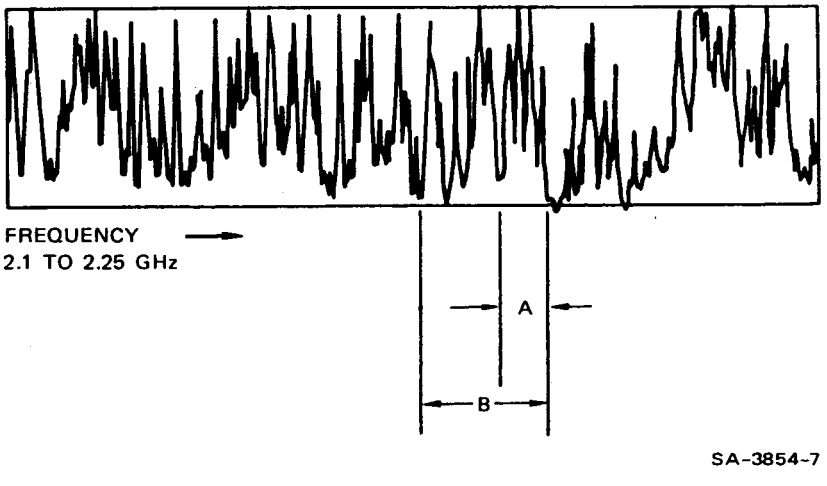

FIGURE 8 REPRESENTATIVE DETECTED MODE PATTERN.
Source: Figure 4-10, Reference 5.

are "riding" on a mode of substantially lower Q_L--that is, a mode whose width is roughly A. The correct count for frequency interval A should then be five.

Similarly, visual inspection of the interval B suggests that, in addition to the several high Q_L modes there are three low Q_L modes (of width about B/3), plus one very low Q_L mode of width $\approx$ B that should be added to the experimental count before it might be compared with the theoretically predicted count.

The foregoing assumes that the supplementary extra low Q_L modes indicated--which are essentially coarse and extra coarse undulations of the base line--are not modes of resonance excluded by the theory (e.g., a resonant ladder) nor are they caused by frequency dependent RF circuit components external to the fuel tank. After verifying that this is not the case, a possible technique for detecting the very low Q_L modes might be based on successive stages of low-pass filtering of the video waveform with supplementary counting provided at each stage to record the number of low Q_L, extra low Q_L, and so on, modes.

F. System Errors

In discussing the errors associated with any measuring system, one must note the distinction between precision and accuracy. If a measuring system exhibits only small random errors, it is said to possess high precision; the accuracy is high, on the other hand, only if the systematic errors are small. Thus, the mean deviation of data points from a "best-fit" curve obtained by regression analysis is a measure only of the precision. The accuracy, however, would be determined if we knew how closely the gauge reading agreed with the actual amount of fuel in the tank. Thus, the accuracy will depend on the way the gauge is calibrated and on whether any systematic changes in mode count can

occur that are not related to the amount of fuel in the tank. For example, empty-cavity mode count shifts of 25% have been observed by Bendix. The occurrence of such a shift in an operating system would result in a significant change in the fuel gauge reading. Figure 4 shows that, when there is a small amount of fuel in the tank, the resulting percentage error can be very large. Obviously, therefore, such systematic shifts in mode count cannot be tolerated in a working system.

IV CONCLUSIONS AND RECOMMENDATIONS

In this study, both theoretical and practical aspects of the Bendix RF fuel-gauging system were examined. The Bendix technique of counting electromagnetic modes of resonance appears to be both a valid and a feasible way for gauging fuel in large space-vehicle fuel tanks. Also, the design and implementation of the fuel-gauging system does, in general, follow the basic tenets of good microwave practice. However, the system does have some limitations which are important to understand. These limitations, as well as a few recommendations for changes in practical technique, are discussed below:

- The coupling to the cavity should be adjusted so that the "under coupled" condition will predominate over the frequency range of interest. This condition will provide the greatest probability of observing a mode, assuming that the detector and mode processor have adequate sensitivity.

- The data processing techniques in use by Bendix will introduce mode-counting errors if: (1) there are some very low Q_L modes intermingled with the more prevalent high Q_L modes, or (2) correct procedures are not used in consideration of the fact that the individual probes in the "space-diversity" probe may each couple to different numbers of modes. To count the low Q_L modes, if they are present, would require additional steps in processing. To avoid errors caused by misinterpretation of diversity probe action, the video waveforms should be summed before the modes are counted.

- Since the cavity dimensions are all so very large compared with a wavelength, the addition of perturbations to the cavity should have very little effect on the average number of degeneracies that occur in a given frequency range.

- Transient changes in the loaded-Q--such as might be produced by changes in losses, coupling, or movement of the dielectric fluid--should not significantly affect the gauging response unless they produce so drastic a change in the average loaded Q that mode counting capability is altered. If such effects are found experimentally to be significant, they must somehow be made negligible by making appropriate design changes, if the gauging system is to be practical.

- Temperature effects are difficult to predict: they depend on the kinds and amounts of material that are in the cavity and their relative contributions to the overall loss and dielectric filling factor. Although one can take steps to minimize the use of temperature sensitive materials within the cavity, one should also always maintain the temperature constant (at the expected operating temperature) during calibration (assuming the temperature during flight is constant).

- The Bendix math model appears to apply to only one of the many possible distributions of loaded-Q values that might be found for the modes in a frequency range (f_1, f_2). A suggested modification of the Bendix model is presented that should make it possible to account for any distribution of loaded-Q values.

- A normalized frequency variable is introduced, which leads to a simple set of criteria for determining the general type of gauging response to be expected and, hence, the most desirable operating frequency range.

- The theory is expected to be the least accurate for nearly empty and nearly full cavities, with the probability for the occurrence of large percentage errors being highest in the case where the cavity is nearly empty.

- For the new model, it is found that the unloaded, external, and loaded Qs of the empty cavity should be measured for most of the modes in the frequency range (f_1, f_2) if accurate values for the model parameters are to be determined.

- Also, in the model, the effect of mode degeneracies can only be approximated. However, since the detailed cavity geometry in the large cavity approximation should not affect the average number of degeneracies, it should be possible to account for degeneracies by a suitable calibration.

- Similarly, modes may go undetected if there is insufficient coupling. Coupling variations from mode to mode occur because of differences in the modal field configurations. The use of a "space-diversity" probe by Bendix is considered to be a good technique for alleviating this problem. The optimum design of the probe must be determined empirically, but the design should not be sensitive to the position of the probe in the cavity.

- Although the model should provide a good basis for design, its accuracy is probably not good enough to eliminate the need for experimentally calibrating the actual fuel-gauging system.

Appendix A

INTEGRATION OF A FERMI-TYPE MODE DENSITY FUNCTION

Appendix A

INTEGRATION OF A FERMI-TYPE MODE DENSITY FUNCTION

We wish to evaluate the integral

$$J(\eta') = \int_0^{\eta'} \frac{\eta^2 d\eta}{1 + e^{\gamma(\eta-1)}} \quad . \tag{A-1}$$

To simplify the exponent we set

$$t = \frac{\gamma}{2} (\eta - 1) \quad . \tag{A-2}$$

Hence,

$$\eta = \frac{2t}{\gamma} + 1 \quad . \tag{A-3}$$

Equation (A-1) then becomes

$$J(\eta') = \frac{2}{\gamma} \int_{-\frac{\gamma}{2}}^{-\frac{\gamma}{2}(\eta'-1)} (1 + 2t/\gamma)^2 \, (1 - \tanh t)dt \quad , \tag{A-4}$$

which can be written as

$$J(\eta') = \frac{(\eta')^3}{6} + \frac{1}{\gamma} \ell n \frac{\cosh \gamma/2}{\cosh \gamma(\eta'-1)/2}$$

$$- \frac{4}{\gamma^2} \left\{ J_1[\gamma(\eta'-1)/2] - J_1(-\gamma/2) \right\} \qquad \text{(A-5)}$$

$$- \frac{4}{\gamma^3} \left\{ J_2[\gamma(\eta'-1)/2] - J_2(-\gamma/2) \right\} \quad ,$$

where

$$J_k(u) = \int_0^u t^k \tanh t \, dt, \quad k = 1, 2 \quad . \qquad \text{(A-6)}$$

These integrations can be carried out once tanh t is expanded in a series. We must consider two regions of convergence:

(1) Near the origin

$$\tanh t = \sum_{n=1}^{\infty} (-1)^{n-1} \beta_{2n-1} t^{2n-1} \quad , \quad |t| < \frac{\pi}{2} \qquad \text{(A-7)}$$

where

$$\beta_{2n-1} = 2^{2n}(2n^{2n} - 1)B_{2n-1}/(2n)! \qquad \text{(A-8)}$$

The coefficients B_{2n-1} are the Bernoulli numbers, for example,

$B_1 = 1/6$, $B_3 = 1/30$, $B_5 = 1/42$

$B_7 = 1/30$, $B_9 = 5/66$, $B_{11} = 691/2730$,

$B_{13} = 7/6$, etc.

The expansion coefficients are, therefore, given by

$$\beta_1 = 1, \qquad \beta_3 = 1/3, \qquad \beta_5 = 2/15$$

$$\beta_7 = 17/315, \qquad \beta_9 = 62/2835, \qquad \beta_{11} = 1382/155925,$$

$$\beta_{13} = 21844/6081075, \quad \text{etc.}$$

Thus, we can write Eq. (A-6) as

$$J_k(u) = \sum_{n=1}^{\infty} (-1)^{n-1} \beta_{2n-1} u^{2n+k}/(2n + k) \qquad \text{(A-9)}$$

where K = 1, 2 and $|u| \leq 1/2$. Over this range of u (i.e., t) we find that use of the first seven terms of the series provides five decimal place accuracy.

(2) Large, positive t

$$\tanh t = 1 + 2\sum_{n=1}^{\infty} (-1)^n e^{-2nt} \quad . \qquad \text{(A-10)}$$

Now

$$\int_{1/2}^{u} t\, e^{-2nt}\, dt = \frac{(1 + n)e^{-n} - (1 + 2nu)e^{-2nu}}{4n^2} \qquad \text{(A-11a)}$$

and

$$\int_{1/2}^{u} t^2 e^{-2nt}\, dt = \frac{(2 + 2n + n^2)e^{-u} - (2 + 4nu + 4n^2u^2)e^{-2nu}}{8n^3} \quad . \qquad \text{(A-11b)}$$

Therefore, for $u > 1/2$

$$J_1(u) = J_1(1/2) + u^2/2 - 1/8$$

$$+ \frac{1}{2}\sum_{n=1}^{\infty} (-1)^n \frac{(1 + n)e^{-n} - (1 + 2nu)e^{-2nu}}{n^2} \quad , \qquad \text{(A-12)}$$

and

$$J_2(u) = J_2(1/2) + u^3/3 - 1/24$$

$$+ \frac{1}{4}\sum_{n=1}^{\infty} (-1)^n \frac{(2 + 2n + n^2)e^{-u} - (2 + 4nu + 4n^2u^2)e^{-2nu}}{n^3} \quad . \qquad \text{(A-13)}$$

Taking twelve terms of these series gives five decimal place accuracy.

If $u < -1/2$, we have

$$J_k(u) = (-1)^k J_k(-u) \quad , \qquad \text{(A-14)}$$

where $k = 1, 2$.

Appendix B

AUTOMATIC NETWORK ANALYZER Q-MEASURING TECHNIQUES FOR A MULTIRESONANT CAVITY

Appendix B

AUTOMATIC NETWORK ANALYZER Q-MEASURING TECHNIQUES FOR A MULTIRESONANT CAVITY

SRI has had extensive experience in the use of automatic network analyzers (ANA), such as the HP 8541A and 8542B, to measure and display the Q-parameters (unloaded Q, Q_u; external Q, Q_c; and loaded Q, Q_L) of cavity resonators having a multiplicity of resonances. The resonators studied and tested at SRI (under RADC Contracts F30602-71-C-0255 and F30602-74-C-0142) belonged to bandpass filters and the Q-measuring techniques are discussed in detail in the appended list of publications. A summary of these techniques is given below. Note that in the SRI filters only one resonance may exist at a time, whereas in the NASA fuel tanks all the resonances coexist. This difference will not affect the Q-measuring techniques appreciably, however, and only small changes in the computer software would be needed to deal with this difference.

A less important difference between the systems is that the SRI filters all have two separate ports, whereas the fuel tank cavities generally have had only one port. However, attachment of a circulator or directional coupler to the fuel tank RF input creates an effective output port. Alternatively, with the "diversity" RF probe, one element can be used for an input port and any other element for an output port. (Connections from the ANA would be made to the probe elements on the cavity side of the sampling switches). The tightness of coupling at each port can be entirely arbitrary and the insertion loss at resonance, from port to port, is unimportant here, provided it is measurable.

1. HP 8541A ANA

Here, the phase shift from port to port through the filter is noted. This phase shift will have a characteristic value (defined as phase zero) whenever the frequency is centered on a resonance. The frequency of the ANA signal source is made to lock at this frequency, f_0, while f_0 is measured with a digital, precision frequency counter. The insertion loss, L_0, and the VSWR at each port are also measured at f_0. Next, the ANA signal source is made to lock successively onto the frequencies f_1 and f_2 for which the phase shift is +45° and -45°. The frequency counter also measures f_1 and f_2 and sends its readings, along with f_0, back to the computer. The computer then works with the following relations (in which the subscripts 1 and 2 on VSWR and Q_e denote the two ports)

$$Q_L = \frac{f_0}{f_2 - f_1} \tag{B-1}$$

$$L_0 = 10 \log_{10} \frac{Q_{e1} Q_{e2}}{4Q_L^2} \tag{B-2}$$

$$\frac{1}{Q_L} = \frac{1}{Q_{e1}} + \frac{1}{Q_{e2}} + \frac{1}{Q_u} \tag{B-3}$$

$$VSWR_1 = \frac{Q_u + Q_{e1}}{Q_u} \tag{B-4}$$

$$VSWR_2 = \frac{Q_u + Q_{e2}}{Q_u} \tag{B-5}$$

to calculate and output the desired parameters. The entire process is then repeated (automatically) at the next channel or mode of resonance.

2. HP 8542B ANA

This ANA Contains a frequency synthesizer that generates output test signals whose frequencies are stable and known to within one part in 10^6. In the range 1 to 2 GHz, for example, the test frequency can be stepped in increments as small as 2 kHz. The software one uses then includes a "search" procedure to find mode resonance frequencies, f_0, where insertion loss is a minimum (and $\equiv L_0$); phase locking is not used. Additional searching is also done to find the frequencies, f_1 and f_2, where the insertion loss is equal to L_0 + 3 dB. Along with VSWR measurements made at f_0, the equations above remain relevant, and the three frequencies in Eq. (B-1) should be precise to within 1 part in 10^6. Extra software, for example, also can be (and has been) prepared to signal the presence of a resonance mode curve shape corresponding to two partially merged resonances.

PUBLICATIONS RELEVANT TO AUTOMATIC NETWORK ANALYZER
Q-MEASURING TECHNIQUES FOR A MULTIRESONANT CAVITY

"Electronically Tunable High-Power Filter for Interference Reduction in Air Force Communication Systems," Final Report, RADC Contract F30602-71-C-0255, SRI Project 1201, Stanford Research Institute, Menlo Park, California (June 1972).

W.B. Weir, "Automatic Measurement System for a Multichannel Digitally-Tuned Bandpass Filter," IEEE Trans. Instrum. and Meas., Vol. IM-23, No. 2, pp. 140-148 (June 1974).

A. Karp, "Flauto: A High-Power, High-Q Bandpass Filter with Binary Logic Electronic Tuning," IEEE Trans. Microwave Theory and Tech., awaiting publication.

A. Karp and W.B. Weir, "Recent Advances in Binary-Programmed Electronically-Tunable Bandpass Filters of the 'Flauto' Type," to be presented at 1975 International Microwave Symposium, Palo Alto, California, May 13, 1975.

"UHF Electronically Tunable High-Power Filter," Final Report, RADC Contract F30602-74-C-0142, SRI Project 3321, Stanford Research Institute, Menlo Park, California, April 1975 (in preparation).

REFERENCES

1. J. S. Blakemore, Semiconductor Statistics (Pergamon Press, New York, N.Y., 1962).

2. E. O. Ammann and R. J. Morris, "Tunable, Dielectric-Loaded Microwave Cavities Capable of High Q and High Filling Factor," IEEE Trans. on Microwave Theory and Techniques, Vol. MTT-11, pp. 528-542 (November 1963).

3. "Design, Development, and Manufacture of a Breadboard RF Mass Gauging System," Contract NAS-8-30160, Monthly Progress Report No. 43, p. 8, The Bendix Corporation, Instruments and Life Support Division, Davenport, Iowa (November 1972).

4. "Design, Development, and Manufacture of a Breadboard RF Mass Gauging System," Contract NAS-8-30160, Final Report, Phase B, Vol. I, pp. 63-75, The Bendix Corporation, Instruments and Life Support Division, Davenport, Iowa (November 1974).

5. "Design, Development, and Manufacture of a Breadboard RF Mass Gauging System," Contract NAS-8-30160, Final Report, Phase A, The Bendix Corporation, Instruments and Life Support Division, Davenport, Iowa (January 1972).